International Journal of Peptide Research and Therapeutics (2022) 28:96
https://doi.org/10.1007/s10989-022-10401-5

Anti-fungal Effects and Mechanisms of Action of Wasp Venom-Derived Peptide Mastoparan-VT1 Against *Candida albicans*

Mojtaba Memariani[1] · Hamed Memariani[2] · Zahra Poursafavi[3,4] · Zohre Baseri[5]

Accepted: 28 March 2022 / Published online: 23 April 2022

Abstract

Candida albicans, an opportunistic yeast pathogen, is equipped with a plethora of virulence attributes such as yeast-to-hyphae transition, secreted enzymes, tissue adhesion, and biofilm production. The dearth of effective anti-mycotics together with the emergence of drug-resistant *C. albicans* isolates underscore the need to explore novel anti-fungal agents. Anti-microbial peptides (AMPs) have recently awakened considerable interest as potential therapeutic agents. The intent of this study is to assess anti-fungal effects of Mastoparan VT-1 (MP-VT1), an AMP from the venom of social wasp *Vespa tropica*, against planktonic and biofilm-embedded cells of *C. albicans*. MP-VT1 had a tendency to adopt alpha-helical conformation based on peptide secondary structure prediction and circular dichroism spectroscopy (in 50% trifluoroethanol). The peptide showed MIC values ranging from 2 to 32 µg/mL against 10 clinical strains of *C. albicans*. Notably, a 6-h of exposure to 1 × MFC of MP-VT1 sufficed for total yeast clearance. At fungicidal concentrations, MP-VT1 exhibited slight cytotoxicity towards human dermal fibroblasts. Flow cytometric analysis and fluorescence microscopy revealed that MP-VT1 induced membrane disruption, leading to death of *C. albicans* mainly by necrosis. Interestingly, a significant inhibition of hyphal transition was noticed at 3 and 6 h post-contact with 32 µg/mL of MP-VT1. At sub-lethal concentrations, the peptide lessened not only candidal cell surface hydrophobicity but also the number of yeasts adhering to the polystyrene surfaces. Furthermore, *C. albicans* cells within biofilms were more vulnerable to MP-VT1 than to fluconazole. Overall, MP-VT1 has the potential to be used as a candidate for anti-fungal drug development.

Keywords *Candida albicans* · Mastoparan-VT1 · Biofilm · Cell surface hydrophobicity · Necrosis

Abbreviations

AMPs	Anti-microbial peptides
AO/EtBr	Acridine orange/ethidium bromide
CD	Circular dichroism
CFUs	Colony forming units
CSH	Cell surface hydrophobicity
DMEM	Dulbecco's Modifed Eagle's Medium
DMSO	Dimethyl sulfoxide
FCS	Fetal calf serum
FITC	Fluorescein isothiocyanate
HFFs	Human foreskin fibroblasts
MFC	Minimum fungicidal concentration
MIC	Minimum inhibitory concentration
MP-VT1	Mastoparan VT-1
MOPS	3-(*N*-Morpholino) propane sulfonic acid
OD	Optical density
PBS	Phosphate-buffered saline
PI	Propidium iodide
RP-HPLC	Reversed phase–high-performance liquid chromatography
RPMI 1640	Roswell Park Memorial Institute 1640
SD	Standard deviation
SDA	Sabouraud dextrose agar
SDB	Sabouraud dextrose broth

✉ Hamed Memariani
h.memariani@gmail.com

1 Department of Pathobiology, School of Public Health, Tehran University of Medical Sciences, Tehran, Iran

2 Biotechnology Research Center, Pasteur Institute of Iran, Tehran, Iran

3 Biology Department, Science and Research Branch, Islamic Azad University, Tehran, Iran

4 Cord Blood Bank, Royan Stem Cell Technology Company, Tehran, Iran

5 Department of Pathology and Laboratory Medicine, Shariati Hospital, Tehran University of Medical Sciences, Tehran, Iran

TFE	2,2,2-Trifluoroethanol
YNBG	Yeast nitrogen base medium containing 2% glucose

Introduction

Candida albicans is an opportunistic yeast pathogen that normally resides in the oral cavity, gut, and genital-urinary tracts of healthy humans (Lohse et al. 2018). Candidiasis encompasses diseases that range from mucosal, manifesting as vaginitis or thrush, to life-endangering systemic infections with a high mortality rate in patients with immune-debilitating comorbidities (Memariani and Memariani 2020). In order to successfully colonize such diverse host niches, *C. albicans* is equipped with a constellation of virulence factors and fitness attributes. As is well-known, morphological switch from yeast to filamentous growth form plays a prominent part in *C. albicans* pathogenesis (Talapko et al. 2021). This transition is triggered in response to multiple environmental signals, including a high pH (> 7), nutrition deprivation, presence of serum or *N*-acetylglucosamine, elevated temperature, high CO_2 concentration, and adherence. The yeast form is perceived to be involved in dissemination of the pathogen, whereas the hyphal phenotype is necessary for not only mucosal invasion but also biofilm formation (Mayer et al. 2013).

A key virulence trait of *C. albicans* is its aptitude to establish biofilms on both abiotic and biotic surfaces. *C. albicans* biofilms are defined as a complex consortium of adherent yeasts and hyphal cells encased in a matrix of extracellular polymeric substances. Indeed, *C. albicans* has a propensity to develop biofilms on implanted medical devices such as catheters, shunts, stents, prostheses, and endotracheal tubes (Lohse et al. 2018). Mature biofilms are notorious for their exceptional resilience to contemporary anti-fungal chemotherapeutics and host immune defenses (Lee et al. 2021).

Therapeutic strategies against *C. albicans* differ substantially depending upon the anatomic location of the infection, the patients' underlying disease, severity of the infection, and, in some cases, the susceptibility of the strains to specific anti-fungal drugs (Talapko et al. 2021). Within the limited anti-fungal armory, azoles still remain the most commonly prescribed agents for candidiasis therapy. Other anti-fungal drugs that are currently approved to cure severe infections include polyenes (e.g., amphotericin B and nystatin), echinocandins (e.g., caspofungin), and 5-flucytosine (Lee et al. 2021). Regrettably, extravagant use of existing anti-fungal agents has led to the rapid emergence and spread of drug-resistant *Candida* species. Along with these problems, the anti-fungal medications have several limitations owing to issues with drug safety profiles, pharmacokinetic properties, untoward side effects, and narrow spectrum activity (Snyder et al. 2021). For these reasons, pharmaceutical industry needs to be actively involved in exploring new sources to ensure a sustainable pipeline of new anti-mycotics.

Venoms are now being considered as an untapped source of novel and potential leads suitable for further drug development. Bee and wasp venoms contain several cationic antimicrobial peptides (AMPs) among which melittin and the mastoparan family have aroused a great deal of scientific interest in fighting against different diseases (Moreno and Giralt 2015; Memariani and Memariani 2021). Melittin, the major constituent in the venom of European honeybee *Apis mellifera*, is a multifunctional peptide with reported anti-bacterial (Lima et al. 2022), anti-biofilm (Memariani et al. 2019), anti-fungal (Choi and Lee 2014), anti-protozoan (Adade et al. 2013), anti-viral (Uddin et al. 2016), anti-cancer (Lyu et al. 2019), anti-inflammatory (Lee and Bae 2016), and anti-diabetic (Hossen et al. 2017) properties. Among the other important venom-derived AMPs are mastoparans. In general, peptides belonging to the mastoparan family are 14 amino acids in length. The majority of mastoparans are replete with hydrophobic residues leucine, isoleucine, valine, and alanine. These peptides possess two to four lysine residues in their primary sequences with a C-terminal amide moiety (da Silva et al. 2014). Multiple biological activities have been attributed to mastoparans (Chen et al. 2018). For example, mastoparans Polybia-MP-II and -III have been shown to contribute to mast cell degranulation, lactate dehydrogenase release from the cytoplasm of mast cells, hemolysis, leukocyte chemotaxis, and inhibition of bacterial growth (de Souza et al. 2009). In addition, different mastoparans exhibit potent anti-cancer activities upon leukemia, glioblastoma, myeloma, and breast cancer cells (Hilchie et al. 2016; da Silva et al. 2018). Given the multifunctionality of some venom-derived peptides, there is still room to explore other unknown activities for these peptides.

Thus far, in vitro studies have dealt predominantly with anti-bacterial activities of mastoparans. For instance, one study (Chen et al. 2018) revealed that mastoparan-C from the European hornet (*Vespa crabro*) venom and its two derivatives possess broad-spectrum activity against planktonic and biofilm-encased bacteria. In another study, mastoparan and three of its analogues displayed pronounced anti-bacterial activity toward four extended drug-resistant *Acinetobacter baumannii* isolates (Vila-Farrés et al. 2015). Furthermore, Polybia-MP-II has been demonstrated to be effective against various Gram-positive and Gram-negative bacteria (de Souza et al. 2009). Nevertheless, only meager data exist pertinent to fungicidal properties of mastoparans (El-Wahed et al. 2021). This prompted us to evaluate anti-fungal effects of mastoparan VT-1 (MP-VT1), a tetradecapeptide isolated from the venom of social wasp *Vespa tropica* (Yang et al. 2013), against both planktonic and biofilm-embedded cells

of *C. albicans*. We further addressed the question of whether the peptide would influence yeast-to-hyphae transition in *C. albicans*. The possible toxicity towards human fibroblasts was also assessed in our experiments.

Materials and Methods

Reagents and Media

All common reagents used in the current study were of analytical grade from commercial suppliers. Agar–agar, 2,2,2-trifluoroethanol (TFE), and yeast extract were procured from Merck Co. (Darmstadt, Germany), while *Candida* chromogenic agar was purchased from Conda Laboratorios (Madrid, Spain). Roswell Park Memorial Institute (RPMI) 1640 medium, Dulbecco's Modifed Eagle's Medium (DMEM), and fetal calf serum (FCS) were supplied by Gibco-BRL (Life Technologies, Ltd., Paisley, Scotland). Annexin V-fluorescein isothiocyanate (FITC)/propidium iodide (PI) staining kit was obtained from IQ Products (Groningen, The Netherlands). The other materials were all supplied by Sigma–Aldrich Chemical Co. (Steinheim, Germany).

Peptide Synthesis

C-terminally amidated MP-VT1 (INLKAIAALAKKLL—NH_2) was manufactured at Mimotopes Company (Clayton, Victoria, Australia) employing the Fmoc/*t*-butyl solid phase synthesis strategy (Smart et al. 1996). Purification of MP-VT1 was carried out by analytical reversed phase-high performance liquid chromatography (RP-HPLC) using a C18 column (4.6 × 150 mm). Samples were run at a flow rate of 1.5 mL/min utilizing a mobile phase encompassing 0.1% trifluoroacetic acid in 100% H_2O (solvent A) and 0.1% trifluoroacetic acid in 90% acetonitrile (solvent B) with the following gradient program: 10% B for 1 min; 10–66.6% B (linear) over 15 min; then column re-equilibration. Analysis of the chromatograms is performed and retention time (RT, min) is then recorded by Empower™ 2 software Build 2154 at λ = 214 nm. Mass spectrometry on a Perkin Elmer Sciex API III (Norwalk, CT, USA) and its accompanying software were used to validate peptide identity. The mass spectrometer was operated in the positive mode. Moreover, the eluent was 0.1% acetic acid in 60% acetonitrile. The purified MP-VT1 was lyophilized and stored at − 40 °C.

Peptide Secondary Structure

The secondary structure of MP-VT1 was predicted online utilizing SABLE protein prediction (https://sable.cchmc.org) server, which possessed a mean prediction accuracy about 80% (Adamczak et al. 2005).

Circular dichroism (CD) spectra of MP-VT1 in water either in the presence or absence of 50% (*v*/*v*) TFE were recorded in a 1-mm path-length quartz cuvette at 24 ± 2 °C on an AVIV MODEL 215 spectropolarimeter (AVIV Instruments, Inc., Lakewood, NJ, USA) over a wavelength range of 190–260 nm, as detailed elsewhere (Memariani et al. 2018). The mean residue molar ellipticity ([θ]) was calculated as follows:

$$[\theta] = \frac{\theta}{10 \times l \times c_M \times n}$$

where θ, l, c_M, and n represent the ellipticity, the optical path length of the cuvette, MP-VT1 concentration, and the number of amino acid residues in MP-VT1, respectively (Lee et al. 2003). CDNN 2.0 software (Gerald Böhm, Martin-Luther-Universität Halle-Wittenberg, Germany) was also used to quantify secondary structure contents of the peptide.

C. albicans Strains and Culture Conditions

Ten clinical strains of *C. albicans* (Table 1) were included in the current study. *Candida* chromogenic agar, germ tube formation, and VITEK® MS (bioMérieux, Marcy l'Etoile, France) were used for identification of the *C. albicans* strains (Walsh et al. 2018). *C. albicans* ATCC 90028 was employed as a quality control strain. Before each experiment, the strains were revived from − 80 °C stocks by sub-culturing twice onto Sabouraud dextrose agar (SDA) for 48 h. A loopful of a single colony from SDA was then transferred to Sabouraud dextrose broth (SDB) and incubated at 35 °C for 8 h. After centrifugation, each strain was adjusted to a cell density of 10^6 cells/mL with PBS unless otherwise indicated.

In Vitro Anti-fungal Activity

The individual minimum inhibitory concentration (MIC) values for planktonic *C. albicans* cells were appraised by broth microdilution assay based upon Clinical and Laboratory Standards Institute guidelines (CLSI 2017), with minor modifications. Succinctly, two-fold serial dilutions of either MP-VT1 or fluconazole were added to wells of flat-bottomed microplates containing 5×10^3 cells/mL in 3-(*N*-morpholino) propane sulfonic acid (MOPS)-buffered RPMI 1640 medium. Microplates were then incubated at 37 °C for 24 h. Wells devoid of drug and yeast cells

Table 1 Anti-fungal activities of mastoparan VT-1 and fluconazole against *C. albicans* isolates

Isolate ID	Isolation period	Source	MP-VT1				Fluconazole			
			MIC[b]	MFC[c]	R[d]	AI[e]	MIC	MFC	R	AI
ATCC 90028	-	Reference strain	16	32	2	FC[f]	0.5	1	2	FC
*Ca*01	2021, Q1[a]	Urinary tract	16	16	1	FC	1	2	2	FC
*Ca*02	2021, Q2	Respiratory tract	4	4	1	FC	8	32	4	FC
*Ca*03	2021, Q2	Urinary tract	8	8	1	FC	4	4	1	FC
*Ca*04	2021, Q1	Wounds/skin/soft tissue	16	16	1	FC	8	16	2	FC
*Ca*05	2021, Q2	Urinary tract	16	16	1	FC	4	16	4	FC
*Ca*06	2021, Q2	Urinary tract	16	16	1	FC	64	128	2	FC
*Ca*07	2021, Q1	Respiratory tract	2	4	2	FC	2	16	8	FS[g]
*Ca*08	2021, Q1	Wounds/skin/soft tissue	8	32	4	FC	16	64	4	FC
*Ca*09	2021, Q1	Blood	32	32	1	FC	16	32	2	FC
*Ca*10	2021, Q2	Urinary tract	8	8	1	FC	2	4	2	FC

[a]Q, Quarter

[b]MIC, Minimum inhibitory concentration (μg/mL)

[c]MFC, Minimum fungicidal concentration (μg/mL)

[d]R, MFC/MIC ratio

[e]AI, Anti-fungal activity index

[f]FC, Fungicidal activity

[g]FS, Fungistatic activity

served as growth and sterility controls, respectively. The MIC was recorded as the lowest drug concentration that elicited 100% inhibition of growth. The minimum fungicidal concentration (MFC) value was also determined by inoculating 10 μL of suspensions from visually clear wells onto SDA plates and subsequent incubation at 37 °C for 24 h. The MFC was defined as the lowest drug concentration to kill at least 99.9% of the starting inoculum. Given that some experiments required a higher number of yeast cells, we also determined the MIC and MFC values for *C. albicans* suspensions at the cell density of 10^6 cells/mL.

Determination of Anti-fungal Activity Index

To understand if MP-VT1 and fluconazole act as fungicidal or fungistatic agents towards *C. albicans* strains, the following ratio was used (Dudiuk et al. 2019):

$$\text{Anti-fungal activity index} = \frac{\text{MFC}}{\text{MIC}}$$

The anti-fungal activity index was defined as follows: fungicidal activity: MFC/MIC ≤ 4, fungistatic activity: 4 < MFC/MIC < 32, and tolerance: MFC/MIC ≥ 32.

Time-Kill Kinetics Assay

To evaluate the pharmacodynamics of the peptide (1/2 × MFC and 1 × MFC), killing activity against *C. albicans* ATCC 90028 was monitored during 6 h exposure (Lum et al. 2015). For this purpose, an initial inoculum of 5×10^3 cells/mL in RPMI 1640–MOPS medium was separately incubated at 37 °C with MP-VT1 and fluconazole. Aliquots (100 μL) were taken at specified time points, diluted 1:10 in pre-warmed phosphate-buffered saline (PBS), and plated onto SDA plates. Finally, resultant colonies were counted after incubation of plates at 37 °C for 24 h.

In Vitro Cytotoxicity on Human Cells

Cytotoxic activity of MP-VT1 against Hu02 cell line (the human foreskin fibroblasts; HFFs) was appraised by means of MTT colorimetry (Memariani et al. 2020). HFFs grown in DMEM supplemented with 10% FCS and 1% penicillin/streptomycin were seeded at 10^4 cells/well for 24 h in 96-well flat-bottomed microplates before being treated with two-fold serial dilutions of MP-VT1. Triton X-100 (0.1%; *v*/*v*) served as a positive control. Microplates were then incubated at 37 °C for 24 h under 5% CO_2 atmosphere. Next, 15 μL of MTT (5 mg/mL in PBS) was pipetted into each well and allowed to react with the cells at 37 °C in darkness for 4 h. After removing the medium and adding dimethyl sulfoxide (DMSO; 100 μL/well), the microplate was gently shaken to facilitate solubilization

of the formazan crystals. The absorbances were read at 570 nm. Finally, the percentage of cell viability was calculated in accordance with the following formula:

$$\text{Cell viability } (\%) = \left[\frac{(S-B)}{(C-B)}\right] \times 100$$

where *S*, *C*, and *B* denote the absorbance of the peptide-treated well, the negative control (i.e. peptide-free well), and the background (i.e. MTT solution with DMEM only), respectively.

Calculation of cell selectivity index

To examine the safety of MP-VT1 in vitro, its selectivity toward the microbial and human cells should be considered. This selectivity can be determined by a simple parameter referred to as "cell selectivity index" (CSI). The higher the CSI, the greater the separation between untoward effects and desired anti-microbial properties. CSI was calculated according to the following equation (Raja et al. 2017):

$$\text{CSI} = \frac{\text{CC}_{50}}{\text{GM}}$$

where CC_{50} signifies the concentration of MP-VT1 required to reduce human fibroblast cell viability by 50% after 24 h and GM denotes the geometric mean of MIC values from all *C. albicans* strains.

Live/Dead Double Staining Assay

Acridine orange/ethidium bromide (AO/EtBr) staining and subsequent fluorescence microscopy were employed to visualize live and dead yeast cells after exposure to MP-VT1 (Memariani et al. 2020). To this end, exponentially growing cultures of *C. albicans* ATCC 90028 were diluted to 10^6 cells/mL and transferred to 0.2-mL opaque microcentrifuge tubes encompassing 1 × MFC or 2 × MFC of MP-VT1. Fluconazole was also used as a comparator anti-fungal drug. After incubation at 37 °C for 4 h, 5 µL of dye mixture (100 µg/mL AO and 100 µg/mL EtBr in distilled water) was mixed with 25 µL of yeast cell suspension on a clean microscope slide before being inspected under a fluorescence microscope (Carl Zeiss AG, Oberkochen, Germany). In an attempt to calculate the percentages of surface area covered by stained yeast cells, fluorescence images were processed through ImageJ software (NIH, rsb.info.nih.gov/ij/). The yeast cells were also divided into two populations, those with green fluorescence (live) and those with orange-red fluorescence (dead).

Assessment of Yeast Cell Death Modes

Annexin V-FITC/PI staining and subsequent flow cytometric analysis of yeasts were chosen to study the physiology and mode of *C. albicans* cell death in response to peptide exposure. Briefly, protoplasts of *C. albicans* ATCC 90028 were discretely exposed for 6 h to 1/4 × MFC (16 µg/mL), 1/2 × MFC (32 µg/mL), and 1 × MFC (64 µg/mL) of MP-VT1 at 37 °C, washed with calcium buffer, and re-adjusted to 10^6 cells/mL in the same buffer (Cho and Lee 2011). Annexin V-FITC (10 µL) was promptly added to the aforesaid suspension, and kept on ice for 15 min in darkness. The cells were washed with calcium buffer prior to being incubated with PI for at least 10 min on ice. The percentage of apoptotic/necrotic cells was analyzed using a PAS II flow cytometer (PARTEC, Münster, Germany).

Yeast-to-Hyphae Switch Assay

To decipher whether MP-VT1 is capable of restraining the morphological switch from yeast to hyphae, 10^6 cells/mL of *C. albicans* ATCC 90028 were grown in RPMI 1640 medium supplemented with 20% FCS in the presence (i.e. sub-MFCs) or absence of MP-VT1 and incubated at 37 °C for 3 and 6 h, after which the yeast-to-hyphae transition was scrutinized by an inverted microscope (Nikon, Eclipse TS100, Tokyo, Japan). Non-treated cells grown in the absence or presence of FCS were used as yeast morphology control and hyphal morphology control, respectively. Amphotericin B served as a comparator anti-fungal drug. At least three aliquots from each experimental condition ($n = 5$) were examined in order to reckon up the percentage of yeast-to-hyphae transition. To calculate this, the following formula was used (Le Lay et al. 2008):

$$\text{Yeast-to-hyphae transition}(\%) = \left[\frac{H}{(Y+H)}\right] \times 100$$

where *H* signifies the number of hyphae and *Y* denotes the number of yeast cells.

Yeast Cell Surface Hydrophobicity Assay

The ability of yeast cells to adhere to an aliphatic hydrocarbon (*n*-hexane) was used as a measure of their cell surface hydrophobicity (CSH) based upon a partially modified method of that described by Krausova and co-workers (2019). Actively growing cells of *C. albicans* ATCC 90028 were standardized to 5×10^6 cells/mL with PBS (initial optical density at 600 nm; $\text{OD}_{\text{initial}}$), and were separately incubated with sub-lethal concentrations of MP-VT1 at 37 °C for 30 min. The cell suspensions (3 mL) and *n*-hexane (1 mL) were pipetted into sterile screw-capped glass tubes, allowed to stand in the water bath at 37 °C for 10 min to equilibrate,

and then in turn vortexed 2 min. The resulting mixture left undisturbed in the water bath at 37 °C for 30 min to permit the immiscible *n*-hexane and aqueous phases to separate. The lower aqueous phase (1 mL) of each sample was cautiously transferred to the measuring cuvette. Subsequently, OD_{600nm} of aqueous phase was measured (OD_{final}). The percentage of CSH was calculated utilizing the following formula (Vaňková et al. 2020):

$$\text{CSH}\ (\%) = \left[\frac{\text{OD}_{\text{initial}} - \text{OD}_{\text{final}}}{\text{OD}_{\text{initial}}}\right] \times 100$$

Yeast Cell Adhesion Assay

Yeast cell attachment to an abiotic surface (polystyrene) in the presence or absence of MP-VT1 was examined in 96-well, flat-bottomed microplates using a new method. Mid-logarithmic growth phase cells of *C. albicans* ATCC 90028 (10^6 cells/mL) in yeast nitrogen base medium containing 2% glucose (YNBG) were separately incubated with sub-lethal concentrations of MP-VT1 at 37 °C for 90 min under unceasing shaking conditions (80 rpm), followed by aspiration of supernatants for removing non-adherent cells from the wells. Loosely-adherent cells were washed thrice with PBS, and the remaining cells were scraped from the bottom of the wells using a sterile micropipette tip. Dissociated cells (200 µL) were then aspirated from the wells, transferred to new microcentrifuge tubes, gently vortexed for 30 s, serially diluted, and spread over the surface of SDA plates. After incubation at 37 °C for 24 h, the percentage of yeast cell adhesion was quantified as follows:

$$\text{Yeast cell adhesion}\ (\%) = \left[\frac{(\text{CFU}_s)}{(\text{CFU}_c)}\right] \times 100$$

where CFU*s* and CFU*c* are the number of colony-forming units corresponding to peptide-treated well and the negative control (i.e. peptide-free well), respectively.

Killing Activity Against Biofilm-Embedded Cells

To address whether MP-VT1 could lessen the viability of biofilm denizens, an assay relying upon the cellular reduction of MTT was adopted (Lee et al. 2018) with some modifications. Briefly, 200 µL of the suspensions of *C. albicans* ATCC 90028 and two biofilm-forming strains (*Ca*05 and *Ca*08) in YNBG (10^6 cells/mL) were added to the wells. After incubation at 37 °C for 90 min under constant shaking (80 rpm), each well was washed twice with PBS. Fresh YNBG (200 µL) was thereafter added to each well, and the microplate was further incubated at 37 °C for 24 h without shaking. The medium was then replaced with fresh RPMI 1640 medium containing different MP-VT1 concentrations. Following incubation at 37 °C for 24 h, the wells were washed twice with PBS. Next, the cells were incubated with 20 µL of MTT dye solution (5 mg/mL) at 37 °C for 3 h. After rinsing the wells with deionized water and subsequent air-drying, DMSO was added to each well. Finally, the absorbance was measured at a wavelength of 570 nm. The percentage of killing activity against biofilm-embedded cells was measured using following equation:

$$\text{Killing activity}\ (\%) = \left[\frac{(C-B)-(T-B)}{C-B}\right] \times 100$$

where *C* indicates the absorbance of the control wells (non-treated biofilm), *B* denotes the absorbance of the blank wells (no biofilm, no treatment), and *T* signifies the absorbance of the peptide-treated wells.

Statistical Analysis

All assays were carried out in triplicate on two separate occasions, unless otherwise stated. SPSS Statistics 20.0 (SPSS Inc. Chicago, Illinois, USA) was employed for statistical analysis. Quantitative data are given as the mean ± standard deviation (SD). Student's *t* test was used to assess significance of difference among groups. Statistical significance was achieved when $p < 0.05$.

Results and Discussion

Peptide Purity and Authenticity

Characterizing biomolecules such as peptides requires the use of several techniques that measure the specific structural or functional features (Acar et al. 2019). In this study, the synthesized MP-VT1 was purified by RP-HPLC. The purity of this peptide was greater than 95% as estimated by RP-HPLC at 214 nm. Moreover, MP-VT1 showed a retention time of 12.24 min (Fig. S1a). The authenticity of MP-VT1 was also confirmed by mass spectrometry (Fig. S1b). Indeed, it is a chief method for determining the precise mass of peptides (Acar et al. 2019). The theoretical molecular weight of this peptide was calculated to be 1478.9 Da, which is in consonant with that obtained from mass spectrometry analysis (1478.7 Da). This similarity affirms the correctness of peptide synthesis. The observed molecular weight of MP-VT1 in this study is congruent with findings of a previous report in which the same peptide showed a molecular weight of 1480.2 Da (Yang et al. 2013).

Secondary Structure Analysis of the Peptide

MP-VT1 is a cationic amphipathic tetradecapeptide showing a helix-forming tendency based upon secondary structure

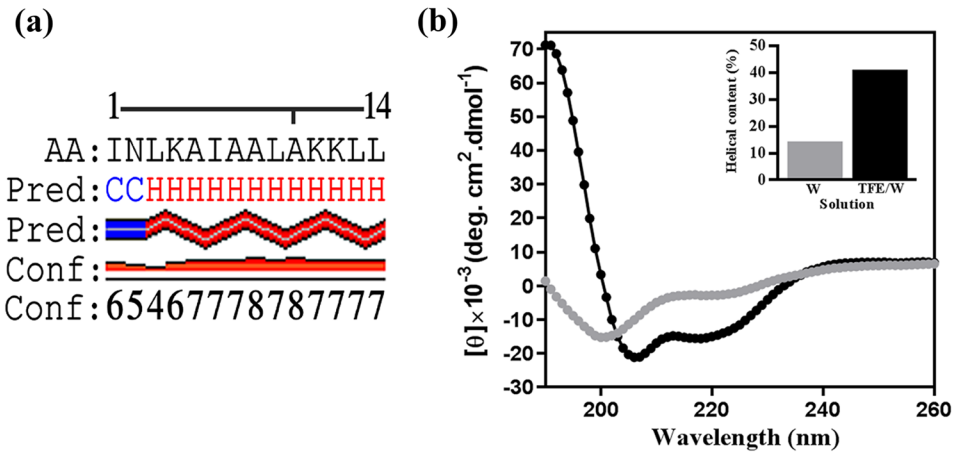

Fig. 1 Secondary structure analysis of MP-VT1. **a** Predicted secondary structure. AA, Pred, and Conf represent single-letter amino acid codes, predicted secondary structure (C; random coil, H; helix), and confidence in the prediction, respectively. **b** Circular dichroism spectra of MP-VT1 in the far-UV region. The spectra recorded for the peptide in water (W) and 50% (*v*/*v*) trifluoroethanol/water (TFE/W) are labeled in gray and black, respectively. Insert represents the helical contents of the peptide

prediction (Fig. 1a). In this context, the majority of amino acid residues of the peptide take the form of helical structure. To further examine the secondary structure of this peptide, the far-UV CD spectra of MP-VT1 were measured in two different solutions (Fig. 1b). In water, the peptide exists predominantly as a random coil, which is deduced by slight shoulder near 220 nm and the trough around 198 nm. Not only is there a double minimum at 222 and 208 nm upon addition of 50% TFE (*v*/*v*) to water, but also the spectrum embodies a maximum at 192 nm; these characteristics are reminiscent of an alpha-helix structure. Comparison of the results of CD analysis with that of the predicted secondary structure shows a satisfactory agreement. The possible reasons behind this active structure could result from the existence of helix-stabilizing residues (e.g., alanine, lysine, and leucine) in the peptide as well as the clustering of hydrophobic residues on one face of the helix (Rončević et al. 2019). We herein selected TFE as the preferred co-solvent because this fluorinated alcohol has been implicated to augment structure formation in peptides and proteins (Culik et al. 2014). In our CD experiments, the helical contents of MP-VT1 in water and 50% (*v*/*v*) TFE/water were 15.2% and 42.0%, respectively. Likewise, Kim et al. (2016) found that four mastoparans behaved as random coils in water, whilst their helical contents increased in response to 40% TFE. The helix-forming tendency is known to be a crucial requirement for mastoparans to display microbicidal activity (Silva et al. 2020).

MIC and MFC Results

C. albicans isolates were originated from urinary tract ($n=5$), respiratory tract ($n=2$), wounds/skin/soft tissue ($n=2$), and blood samples ($n=1$). MIC and MFC values of tested agents against *C. albicans* isolates are shown in Table 1. These values occurred at a cell density of 5×10^3 cells/mL. MIC and MFC values of MP-VT1 against the isolates lied in the range of 2–32 µg/mL, whereas a broader range (0.5–128 µg/mL) was noted for fluconazole. However, the difference between MP-VT1 and fluconazole did not approach statistical significance ($p=0.7910$). The geometric mean MICs of MP-VT1 and fluconazole were calculated to be 12.9 and 11.4, respectively. Moreover, the MFC/MIC ratios of MP-VT1 and fluconazole against almost all *C. albicans* isolates were below or equal to 4, implying that both agents exerted candidacidal activity.

We also evaluated susceptibility of *C. albicans* ATCC 90028 at a higher inoculum size (10^6 cells/mL) to the above-mentioned agents. Using this inoculum size, the MFC value of MP-VT1 (64 µg/mL) was the same as its MIC. In the case of the fluconazole, the MFC (8 µg/mL) was two times the MIC.

Earlier investigations provided evidence for growth-inhibitory activities of several mastoparans and analogues thereof against different *C. albicans* reference strains, typically at MICs ranging from 5 to 80 µg/mL (Galeane et al. 2019; Yang et al. 2013; Wang et al. 2014). It is pertinent to note that experimental variables such as purities of anti-fungal agents, suspending medium used, inoculum sizes, growth media, the age of the culture, and incubation temperature may all influence MIC values (Memariani and Memariani 2020). To our knowledge, susceptibilities of clinical *C. albicans* isolates to mastoparans have hitherto not been examined. By comparison, many studies have used melittin as a comparator anti-fungal peptide for novel or newly discovered peptides. For instance, melittin is highly active against reference and clinical strains of *C. albicans* such as ATCC 10231, ATCC 10261, ATCC 90028, DSM 6659, DSZM 11945, KCTC 7270, and Sc 5314 at MIC range of 0.4–10 µM (Andrä et al. 2001; Andrä and Leippe 1999; Do et al. 2014; Memariani and Memariani 2020; Park et al. 2018; Park and Lee 2009). In spite of potent anti-microbial effects of mastoparans, the anti-fungal efficacy of the

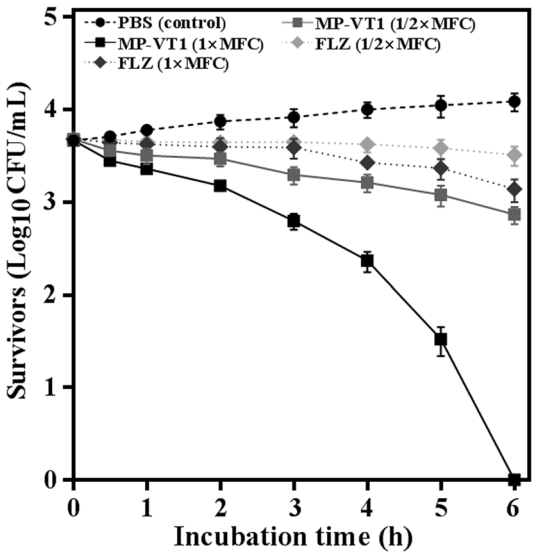

Fig. 2 Killing kinetics of anti-fungal agents against *C. albicans* ATCC 90028. Standardized suspensions of yeasts exposed to different concentrations of either mastoparan VT-1 (MP-VT1) or fluconazole (FLZ) over a period of 6 h. Killing kinetics studies conducted in triplicate on two separate occasions. Each data point represents the mean of data ± SD

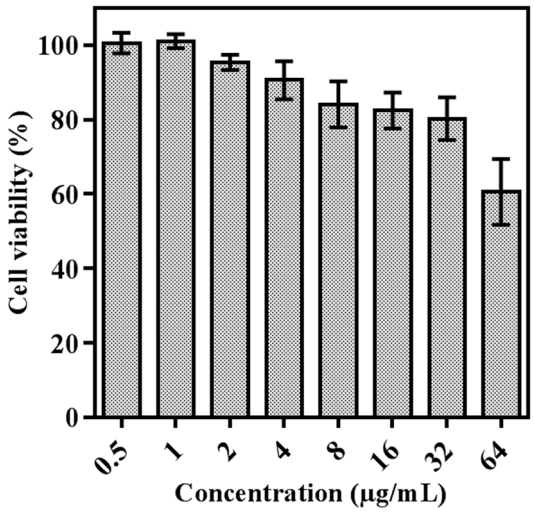

Fig. 3 Cytotoxicity of MP-VT1 against human foreskin fibroblasts (Hu02). The fibroblasts were incubated with ascending concentrations of the peptide for 24 h, after which the percentages of viable cells were determined by use of the MTT assay. Results are expressed relative to the untreated control whose viability was set to 100%. The data are means ± standard deviations of three independent experiments performed in duplicate

peptide in animal models should be further scrutinized in future investigations.

Kinetic Analysis of Yeast Cell Killing

Treatment with MP-VT1 brought about dose- and time-dependent decrements in viability of *C. albicans* cells (Fig. 2). Unlike fluconazole, both 1/2 × MFC (16 µg/mL) and 1 × MFC (32 µg/mL) of the peptide caused appreciable decreases in viable counts after 2 h. These downward rates continued at succeeding hourly intervals. Notably, a 6-h of exposure to 1 × MFC of MP-VT1 sufficed for total clearance of *C. albicans*. However, neither 1/2 × MFC (0.5 µg/mL) nor 1 × MFC (1 µg/mL) of fluconazole eradicated yeast cells within an incubation period of 6 h (Fig. 2). As judged by time-kill measurements, MP-VT1 had faster candidacidal kinetics in comparison to fluconazole. The rapid microbicidal activity of AMPs seems to offer several advantages over conventional anti-fungal drugs including limiting the dissemination of pathogens, improving outcome of the disease, shortening treatment durations, and reducing the likelihood of resistance development (Mohamed et al. 2016).

MTT Assay Results

MTT colorimetric assay was used to gain insight into potential cell toxicity of MP-VT1. As illustrated in Fig. 3, MP-VT1 dose-dependently decreased the viability of HFFs. Within the concentration range of 0.5–32 µg/mL, more than 80% HFFs were still viable after 24 h of treatment (Fig. 3). Such concentrations were indeed enough to eradicate all of the tested *C. albicans* isolates, suggesting selective toxicity of the peptide on *C. albicans* over human fibroblasts. In the present study, however, the peptide exhibited moderate toxicity at 64 µg/mL, reducing the cell viability to 60.53%. The CC_{50} value of MP-VT1 against HFFs was thus greater than 64 µg/mL after incubation for 24 h.

In a recent study, insertion of a pentapeptide motif (FLPII) into the N-terminal extremity of mastoparan L yielded a synthetic peptide mast-MO with decreased toxicity towards mammalian cells and improved anti-microbial activities (Silva et al. 2020). In another work, de Lacorte Singulani et al. (2019) found that a mastoparan analogue MK58911 (INWLKIAKKVKGML-NH_2) at concentrations up to 500 µg/mL showed no toxicity against human fetal lung fibroblasts (MRC5) and glioblastoma cells (U87). Evidently, further investigations will be needed to elucidate the cytotoxic effects of MP-VT1 on other human cell lines.

Cell Selectivity Index

In drug development, it is of importance that a new candidate agent displays a safe therapeutic profile wherein the drug concentration required to attain the desired therapeutic effect is considerably lower than the concentration that incurs cytotoxic effects upon human cells (Porto et al. 2018). High anti-microbial activity (i.e., low MIC value)

together with low cytotoxicity (high CC_{50}) is indeed needed to achieve high CSI. In fact, CSI could be taken as a starting point to decide whether or not to pursue preclinical trials (Memariani et al. 2017). In this study, the GM of MP-VT1 was 12.9 µg/mL against 11 *C. albicans* strains. Given that MP-VT1 did not reduce the viability of HFFs by 50% even at the maximum concentration tested (64 µg/mL) in MTT colorimetric assay, a minimal twofold concentration value was used to calculate the CSI (i.e. $CC_{50} > 64$ µg/mL was considered as 128 µg/mL), as suggested earlier (Raja et al. 2017). In the present study, CSI for the peptide was found to be 9.9, indicating higher specificity of MP-VT1 for fungal cells compared with HFFs. Some authors are of opinion that CSI value should ideally be equal to or above 10 (Indrayanto et al. 2021; Awouafack et al. 2013). In one study, CSI of porcine myeloid anti-microbial peptide-36 (PMAP-36) against fungi was 0.21, while an 18-mer alpha-helical peptide RI18 displayed the greatest cell selectivity (22.61) among shorter derivatives of PMAP-36. However, melittin, a honeybee venom-derived peptide, showed a CSI of 0.07 (Lyu et al. 2016). The selective toxicity of some AMPs like MP-VT1 could be attributed to inherent differences in biomembrane lipid compositions in fungi and mammalian cells. In this context, ergosterol is the main lipid component of fungal cells, while cholesterol is the major neutral lipid in mammalian cells (Wang et al. 2014).

Visualization of Live and Dead Cells

We also performed AO/EtBr double staining method and fluorescence microscopy for direct visualization of live (green fluorescence) and dead (orange-red fluorescence) yeasts. Using this method, it is possible to stain yeast cells with either intact or damaged membrane simultaneously. As expected, a conspicuous green fluorescence was observed in PBS-treated yeast cells (Fig. 4a). The proportion of dead cells increased with peptide dose (Fig. 4b and c). In particular, the number of cells displaying orange-red fluorescence was highest when cells were challenged with 2×MFC (128 µg/mL) of the peptide for 4 h. For comparison, no such changes are evident in fluconazole-treated cells (Fig. 4d and e). After analyzing fluorescence images using ImageJ software, we found that less than 0.10% of the surface area of the negative control image was covered by dead yeast cells (Fig. 4f). Remarkably, the percentages of surface areas covered by dead yeast cells in Fig. 4g and h (1.91% and 5.27%; peptide-treated *C. albicans* cells) were much greater than those found in Fig. 4i and j (0.48% and 0.68%; fluconazole-treated cells). Overall, these observations suggest that MP-VT-1 disrupted cell wall integrity and enhanced cell membrane permeability, resulting in yeast cell death. The changes in viability of the yeasts corroborate the aforementioned data regarding dose-proportional killing effects upon *C. albicans* cells. In line with our observations, previous studies plainly demonstrated that various mastoparans can inflict microbial cell membrane damage in both bacteria and

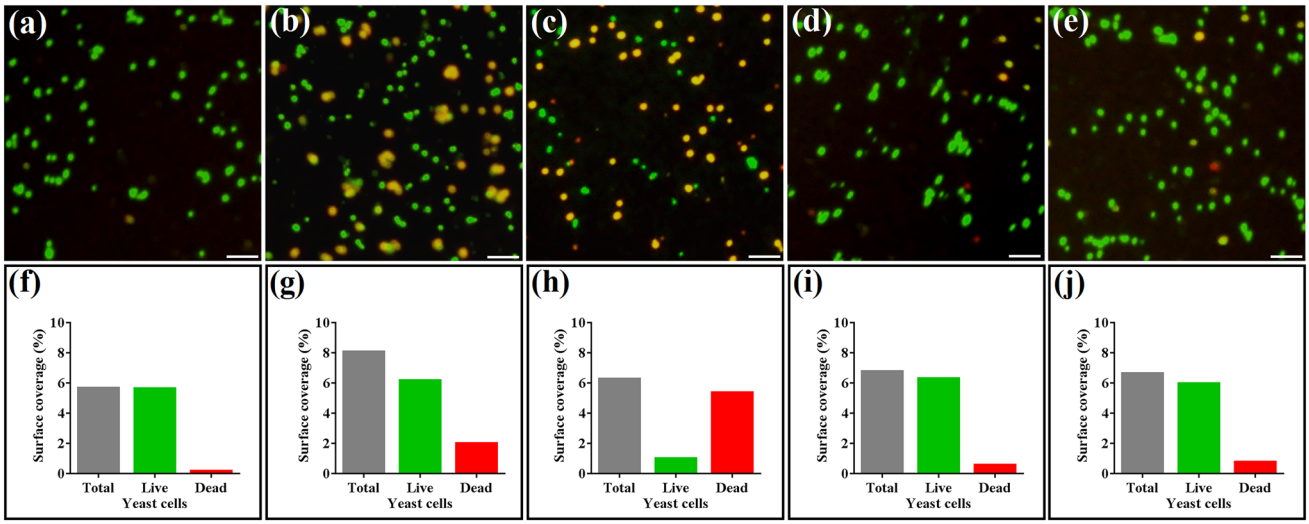

Fig. 4 Fluorescence microscopy images of yeast cells (*C. albicans* ATCC 90028) after exposure to either MP-VT1 or fluconazole for 4 h. AO/EB staining was employed to concomitantly observe live and dead yeast cells (scale bars = 25 µm). PBS-treated yeast cells served as a negative control (**a**). Panels **b** (1×MFC; 64 µg/mL) and **c** (2×MFC; 128 µg/mL) indicate yeast cells that were challenged with MP-VT1, while panels **d** (1×MFC; 8 µg/mL) and **e** (2×MFC; 16 µg/mL) represent fluconazole-treated cells (original magnification: 400x). Panels **f** (negative control), **g** (1×MFC of MP-VT1), **h** (2×MFC of MP-VT1), **i** (1×MFC of fluconazole), and **j** (2×MFC of fluconazole) represent the percentages of surface areas covered by stained yeast cells (i.e. total, live, and dead cells)

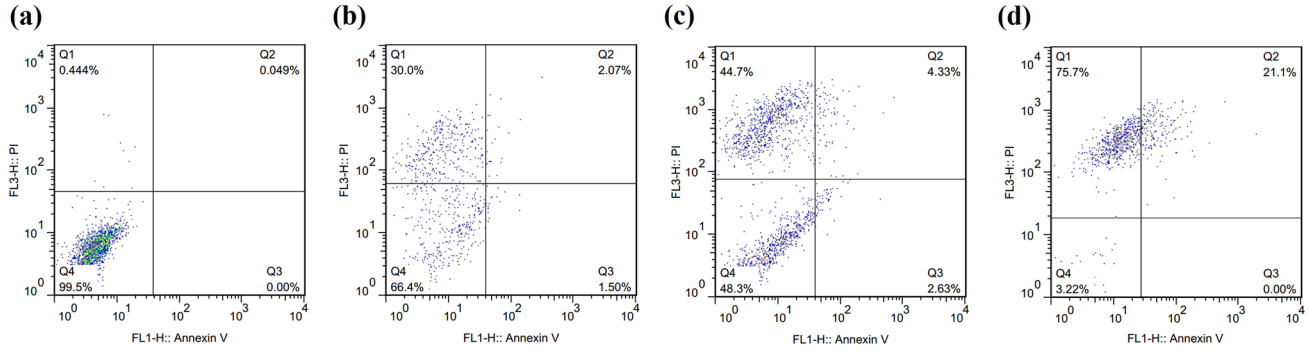

Fig. 5 Flow cytometry dot plots for MP-VT1-exposed yeast cells (*C. albicans* ATCC 90028) stained with Annexin V-FITC/PI. PBS-treated yeasts used as a negative control (**a**). Panels **b**, **c**, and **d** depict yeasts that were treated with 1/4 × MFC (16 µg/mL), 1/2 × MFC (32 µg/mL), and 1 × MFC (64 µg/mL) of MP-VT1, respectively. The yeast cell populations in four quadrants of a quadrant dot plot were interpreted as necrotic/damaged cells (annexin V − /PI + , Q1), late apoptotic (annexin V + /PI + , Q2), early apoptotic (annexin V + /PI − , Q3), and viable cells (annexin V − /PI − , Q4)

fungi, ultimately culminating in cell lysis (de Lacorte Singulani et al. 2019; Silva et al. 2020; Irazazabal et al. 2016).

Analysis of Yeast Cell Death Responses

Having shown that MP-VT1 instigates cell demise in *C. albicans*, we next sought to explore the extent of apoptosis and necrosis in MP-VT1-treated yeast cells. One of the hallmarks of apoptosis is phosphatidylserine exposition which can be detected by annexin V staining and subsequent flow cytometry analyses (Cho and Lee 2011). On the other hand, PI can be applied to inspect cell membrane integrity. In our work, 99.5% of the non-treated yeast cells (control) occupied the lower left quadrant in Fig. 5a; hence, they were detected as viable. When exposed to sub-MFCs of the peptide for 6 h, approximately 30–45% of yeast cell populations underwent necrosis (Fig. 5b and c). Nevertheless, evidence of apoptosis was typically limited to < 7% of the cells treated with sub-MFCs of MP-VT1. At the concentration equal to MFC of the peptide, almost three-quarters of yeast cells displayed necrosis, while a smaller proportion of the population exhibited late apoptosis (Fig. 5d). Therefore, necrosis appears to be a principal mechanism by which MP-VT-1 exterminates yeast cells. Until now, only rarely has the extent of apoptosis/necrosis in fungal cells in response to mastoparan challenge been quantified. In agreement with our findings, a contemporary study (de Lacorte Singulani et al. 2019) indicates that necrosis is the major form of cell death in the basidiomycetous yeast *Cryptococcus neoformans* exposed to MK58911, a mastoparan analogue.

Inhibition of Morphological Switch

It has been suggested that the hyphal growth promotes tissue invasion, bestows protection against host immune cells, and

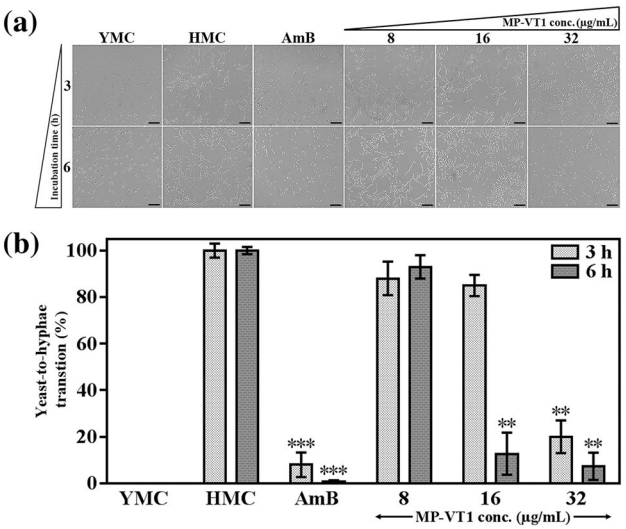

Fig. 6 Effect of MP-VT1 upon *C. albicans* yeast-to-hyphae transition. *C. albicans* ATCC 90028 was cultured in in RPMI 1640 medium plus 20% fetal calf serum with or without MP-VT1 at various concentrations (1/8 × MFC; 8 µg/mL, 1/4 × MFC; 16 µg/mL, and 1/2 × MFC; 32 µg/mL) and maintained for 3 and 6 h at 37 °C. After completion of each culture period, the numbers of yeast and hyphal forms were calculated. **a** and **b** show representative images of *C. albicans* cells obtained using an inverted microscope (scale bars = 50 µm) and the percentages of the cells undergoing morphological switch from yeast to hyphae, respectively. YMC, HMC, and AmB denote yeast morphology control, hyphal morphology control, and amphotericin B, respectively. In **b**, error bars represent the standard deviation of the mean. The asterisks (*) represent statistical significance compared with HMC (*$p < 0.05$, **$p < 0.01$, and ***$p < 0.001$)

facilitates appropriate biofilm establishment (Tsang et al. 2012). Since MP-VT1 inhibited *C. albicans* growth, we hypothesized that the peptide would also attenuate morphogenesis from yeast to hyphae in vitro. In the present work, non-treated *C. albicans* cells exhibited yeast-like phenotypes

in serum-free RPMI 1640 medium after 3 and 6 h (Fig. 6a and b), whereas addition of 20% FCS to the medium resulted in uniform distribution of hyphal cells (Fig. 6a and b). As depicted in Fig. 6b, addition of 1/8 × MIC (8 µg/mL) of MP-VT1 had little inhibitory effects upon *C. albicans* transition at both exposure times. At 1/4 × MIC (16 µg/mL) of the peptide, 85% of *C. albicans* cells underwent hyphal morphogenesis after a 3 h of incubation, while increasing exposure time to 6 h caused a substantial decrement in hyphal morphogenesis as compared with the hyphal morphology control ($p < 0.01$). Interestingly, a significant inhibition of hyphal transition ($p < 0.01$) was noticed at 3–6 h post-contact with 1/2 × MIC (32 µg/mL) of MP-VT1. We further established that amphotericin B (5 µg/mL) effectively abrogated hyphal growth of *C. albicans*. From our data, it can be concluded that MP-VT1 elicits a dose-dependent decrement in *C. albicans* yeast-to-hyphae transition. Insofar as we are aware, this is the first study providing phenotypic evidence for the ability of a member of mastoparan family (MP-VT1) to diminish *C. albicans* hyphal formation in vitro. This finding corroborates the results of other investigations in which venom-derived AMPs (e.g., lasioglossin LLIII and ToAP2) were effective in impeding *C. albicans* morphological shift from yeast to hyphae (Vrablikova et al. 2017; do Nascimento Dias et al. 2020). Indeed, suppressing virulence attributes and locking *C. albicans* in a non-hyphae-forming lifestyle have recently been propounded as a novel paradigm for anti-mycotic therapy (Reen et al. 2016). Therefore, inhibition of the yeast-to-hyphae switch may render *C. albicans* less invasive and more vulnerable to conventional anti-mycotics.

Reductions in Yeast Cell Surface Hydrophobicity

As a cellular biophysical parameter of critical importance, CSH influences both cell-surface and cell–cell interactions, thereby contributing to the fungal virulence (Ellepola et al. 2013). How CSH affects virulence has not been fully explicated. It appears that hydrophobic cells in comparison to their hydrophilic counterparts are more adhesive to both biotic and abiotic surfaces, more germination competent, and less sensitive to phagocytosis (Singleton et al. 2005). It is likely that a small variation in candidal CSH results in a shift from commensal to pathogen and vice-versa (Goswami et al. 2017). Various factors such as cell wall composition, nutrient availability, temperature, and fungal growth phase, and even sub-inhibitory doses of anti-fungal agents may alter candidal CSH (Danchik and Casadevall 2021). Herein, we measured yeast adhesion to *n*-hexane following a brief, single exposure to either MP-VT1 or fluconazole alone. As evinced in Fig. 7, MP-VT-1 lessened the CSHs of *C. albicans* ATCC 90028 in a dose-dependent way. Compared with the control (PBS-treated cells), a significant ($p < 0.01$) decrease in hydrophobicity was observed after a

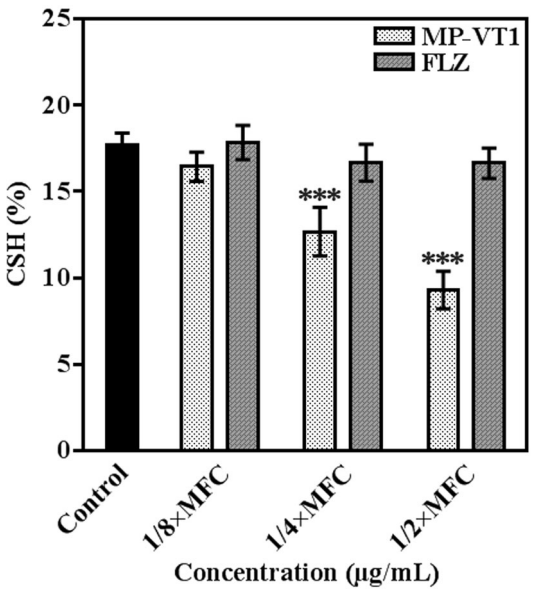

Fig. 7 Effects of mastoparan VT-1 (MP-VT1) and fluconazole (FLZ) on cell surface hydrophobicity (CSH) of *C. albicans* ATCC 90028. Yeast cells were individually incubated with sub-lethal concentrations (1/8 × MFC, 1/4 × MFC, and 1/2 × MFC) of anti-fungal agents at 37 °C for 30 min. The MFC values of MP-VT1 and fluconazole against 5×10^6 cells/mL were 128 and 16 µg/mL, respectively. Error bars show the standard deviation of the mean. The asterisks (*) indicate statistical significance compared with the non-treated control (*$p < 0.05$, **$p < 0.01$, and ***$p < 0.001$)

1-h exposure to either 1/4 × MFC (32 µg/mL) or 1/2 × MFC (64 µg/mL) of MP-VT1. Contrariwise, sub-lethal concentrations of fluconazole had a negligible impact upon yeast CSH (Fig. 7). In congruence with these findings, a recent study (Vaňková et al. 2020) unveiled that 50 µM of a synthetic peptide LL-III/43 (VNWKKILGKIIKVVK-NH_2) efficiently reduced the CSH index of *C. albicans* ATCC MYA-2876, whereas two azoles (i.e. fluconazole and voriconazole) exhibited no significant effect upon the CSH. Different microbial structures such as outer membrane proteins, phospholipids, lipopolysaccharides, fimbriae, and lipopolysaccharide have previously been shown to contribute to microbial CSH (Ellepola et al. 2013). As for *C. albicans*, it has been suggested that the CSH correlates with the concentration of fibrils in the exterior layer of the cell wall (Hazen and Hazen 1992; Ellepola et al. 2013). Therefore, it is sensible to surmise that the reduction of the candidal CSH in the presence of MP-VT1 may be attributable to changes in cell wall surface fibril organization and/or hydrophobic surface proteins. Although our results are interesting, further experiments on medically-significant dimorphic fungi such as *Coccidioides immitis*, *Paracoccidioides brasiliensis*, *Blastomyces dermatitidis*, and *Histoplasma capsulatum* could provide additional insight into the anti-virulent properties of venom-derived AMPs like MP-VT1.

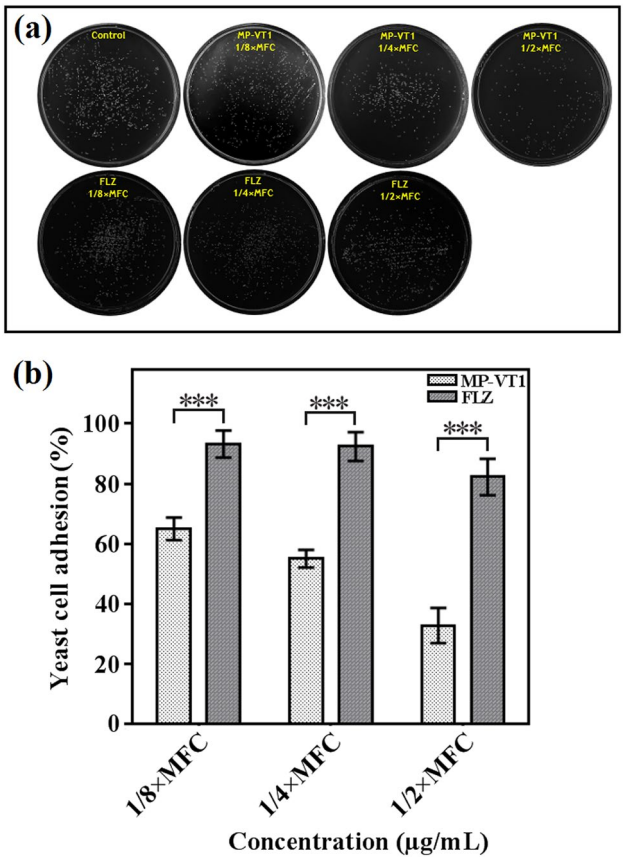

Fig. 8 In vitro yeast cell adhesion assay. *C. albicans* ATCC 90028 cells were permitted to adhere for 90 min in 96-well polystyrene microplates in the presence of sub-lethal concentrations (1/8 × MFC, 1/4 × MFC, and 1/2 × MFC) of either mastoparan VT-1 (MP-VT1) or fluconazole (FLZ). After washing the wells, the remaining cells were resuspended in PBS, serially diluted, spread on SDA plates, and grown for 1 day at 37 °C before quantification on the basis of viable counts. Panels **a** and **b** indicate representative images of yeast colonies and the percentages of yeast cell adhesion in each treatment group, respectively. Results are expressed relative to the control. The data are means ± standard deviations of three independent experiments carried out in duplicate. The asterisks (*) signify significant differences (*$p < 0.05$, **$p < 0.01$, and ***$p < 0.001$) in percentages of yeast cell adhesion between MP-VT1- and FLZ-treated groups

Reductions in Yeast Cell Attachment

Having shown that MP-VT1 is able to diminish candidal CSH, we proceeded to quantify the numbers of polystyrene-attached cells based upon colony counting. Surface attachment is the first step in committing *C. albicans* to the establishment of disease (Fazly et al. 2013). As depicted in Fig. 8a and b, sub-lethal concentrations of both MP-VT1 and fluconazole reduced the adhesion of *C. albicans* ATCC 90028 to polystyrene in a dose-dependent manner. Indeed, in vitro anti-adhesive activity of MP-VT1 was considerably greater than that of fluconazole. Based on our findings, all tested concentrations of MP-VT1 significantly reduced the number of yeasts adhering to the polystyrene surfaces when compared to fluconazole ($p < 0.001$). Remarkably, 1/2 × MFC of MP-VT1 was adequate to inhibit yeast cell attachment by ˃77% (Fig. 8b). A possible explanation may be that MP-VT1 directly binds to cell surface of *C. albicans*, thereby interfering with cell attachment to polystyrene. In this context, the electrostatic affinity between positively charged residues of MP-VT1 and negatively charged membrane carbohydrates may facilitate peptide-cell interactions (Tsai et al. 2011).

Previous studies have indicated that sub-lethal doses of several AMPs such as LL-37, BMAP-28, human β-defensin 3, and histatin 5 inhibit adhesion of *C. albicans* to polystyrene (Tsai et al. 2011; Scarsini et al. 2015). In the case of LL-37, it has been suggested that interaction of the peptide with the yeast cell wall polysaccharides and proteins could affect *C. albicans* adhesion to plastic (Tsai et al. 2011; Chang et al. 2012). Moreover, Brauner and coworkers (2018) have come to realize that the AMP psoriasin binds to the β-glucan of the *C. albicans* cell wall, hence thwarting polystyrene adhesion capacity of *C. albicans*. Prevention of surface attachment by AMPs like MP-VT1 is evidently of importance since they could lessen *C. albicans* colonization and biofilm formation. Nevertheless, it remains unclear what mechanisms are principally responsible for the anti-adhesive activity of MP-VT1. Further studies are therefore needed to address this question.

Fungicidal Effects on Biofilm-Encased Cells

It has been estimated that up to 80% of all human microbial infections are related to biofilms, which are notoriously challenging to treat because of the poor drug penetration, slow growth rate of biofilm populations, altered metabolism of biofilm-encased cells, and over-expression of genes conferring drug resistance (Nobile and Johnson 2015; Olsen 2015). Considering the medical importance of biofilm-associated infections caused by *C. albicans*, we next decided to study whether supra-MFC values of MP-VT1 exhibit fungicidal activity against biofilm-dwelling cells. At concentrations greater than MFCs of MP-VT1 and fluconazole, the viability of *C. albicans* cells embedded in a 24-h biofilm considerably diminished (Fig. 9a and b). As regards *C. albicans* ATCC 90028, more than three-fourths of the biofilm-embedded cells lost their viability after a 24-h exposure to 4 × MFC and 2 × MFC of either MP-VT1 or fluconazole (Fig. 9). Remarkably, peptide concentrations equal to 2 × MFC and 4 × MFC were sufficient to achieve at least 95% reduction in metabolic activity of two clinical biofilm-producer strains, viz. *Ca*05 and *Ca*08 (Fig. 9). However, fluconazole was not as effective as the peptide against those same strains. In particular, a statistically significant difference was found between fungicidal activity of MP-VT1 and fluconazole at 2 × MFC ($p = 0.0001$)

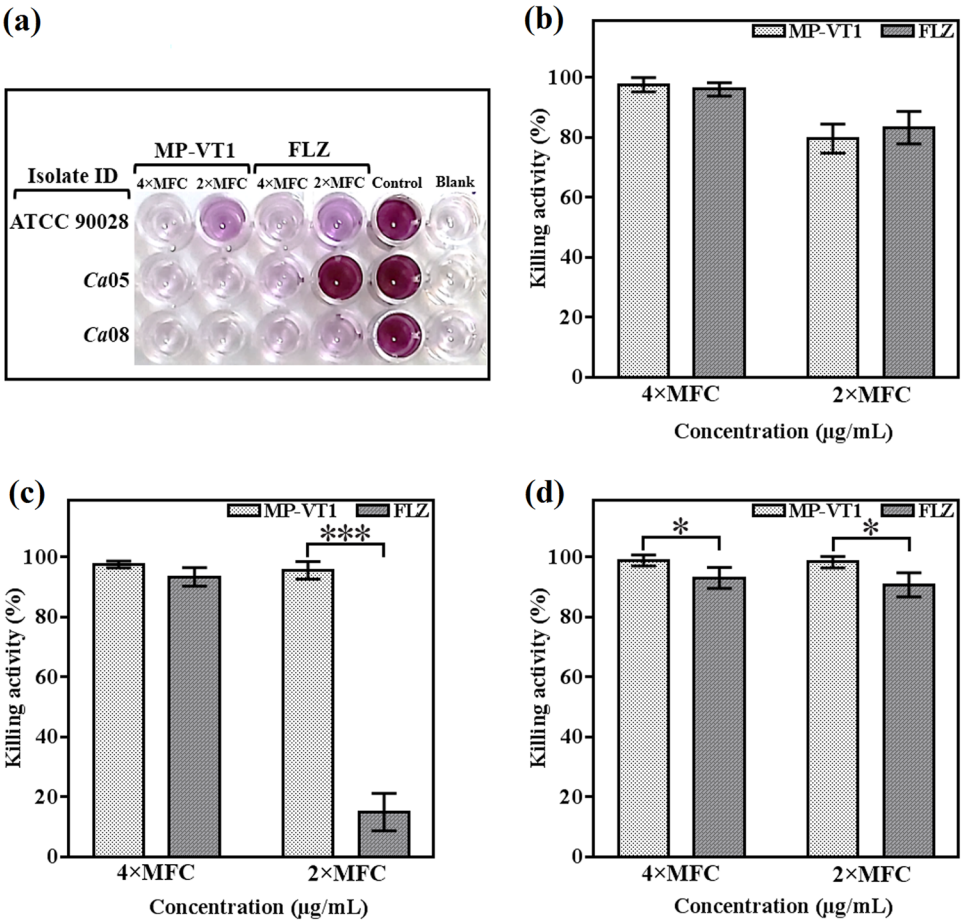

Fig. 9 Fungicidal effects of mastoparan VT-1 (MP-VT1) and fluconazole (FLZ) on biofilm-encased yeast cells. A representative image of wells displaying metabolic activity of biofilm-treated yeast cells is shown in panel **a**. Panels **b**, **c**, and **d** indicate killing activity of anti-fungal agents against *C. albicans* ATCC 90028, *Ca*05, and *Ca*08, respectively. The MFC values of MP-VT1 towards *C. albicans* ATCC 90028, *Ca*05, and *Ca*08 were 64, 32, and 64 µg/mL, respectively. As for FLZ, the MFC values for *C. albicans* ATCC 90028, *Ca*05, and *Ca*08 were 8, 64, and 256 µg/mL, respectively. The data are means ± standard deviations of three independent experiments done in duplicate. The asterisks (*) denote significant differences (*$p < 0.05$, **$p < 0.01$, and ***$p < 0.001$) in percentages of killing activity between MP-VT1- and FLZ-treated groups

against biofilm-embedded cells of *Ca*05. These findings suggest that MP-VT1 could penetrate well inside the biofilm, where it exerts candidacidal activity.

The results of this study bring out that *C. albicans* cells within biofilms are more vulnerable to MP-VT1 than to fluconazole. Similarly, Kočendová et al. (2019) showed that LL-III/43 and VIII, analogues of bee venom-derived peptides, were able to decrease the metabolic activity of different *Candida* spp. cells in mature biofilms at concentrations ranging from 12.8 to 200 µM. In another study, 16 × MFC (128 µg/mL) of lycosin-I, a peptide extracted from the venom of the spider *Lycosa singoriensis*, eradicated not only fluconazole-susceptible but also fluconazole-resistant *Candida tropicalis* biofilms (Tan et al. 2018). It is worthwhile to note that membrane-disrupting activities of some AMPs confer them the ability to act on slow-growing or even non-growing cells including those found at the center of biofilms (Batoni et al. 2011). Hence, AMPs, such as the peptide used in the present study, appear to be promising candidates for the development of novel anti-biofilm agents.

Conclusions

Venom-derived AMPs have recently commanded a great deal of scientific attention, owed partly to their rapid, broad spectrum, and potent anti-microbial activities. The present paper provides us a better understanding of how MP-VT1 exerts its anti-fungal effects upon *C. albicans*. Not only did the peptide obliterate planktonic cells of *C. albicans*, but it also profoundly reduced the viability of biofilm-enclosed cells. Noticeably, MP-VT1 showed faster rates of candidacidal activity as compared to fluconazole. The result of this work suggests that disruption of cell membrane integrity is the principal anti-fungal mechanism of MP-VT-1, culminating in death of *C. albicans* mainly by necrosis. Our study also establishes, for the first time, an inhibitory role for MP-VT1 against virulence attributes of *C. albicans* including yeast-to-hyphae phenotype switching and adhesion ability. We envisage that suppressing virulence behavior of *C. albicans* by MP-VT1 could render the pathogen less invasive and more vulnerable to conventional anti-mycotics. Although the data reported herein reflect the in vitro activity of MP-VT1, future research should scrutinize efficacy of the

peptide in animal models of *Candida* infections to broaden our knowledge on its possible therapeutic effects.

Supplementary Information The online version contains supplementary material available at https://doi.org/10.1007/s10989-022-10401-5.

Author Contributions MM and HM jointly contributed to all phases of this study (conception, experimental design, data analysis, practical work, and authorship of the manuscript). ZP and ZB partially participated in practical work. HM critically reviewed and edited the manuscript. All authors read and approved the final manuscript.

Declarations

Conflict of interest The authors declare that they have no competing interests.

Ethical Approval The manuscript does not contain experiments involving animal or human studies.

References

Acar T, Pelit Arayıcı P, Ucar B, Karahan M, Mustafaeva Z (2019) Synthesis, characterization and lipophilicity study of *Brucella abortus*' immunogenic peptide sequence that can be used in the future vaccination studies. Int J Pept Res Ther 25(3):911–918. https://doi.org/10.1007/s10989-018-9739-0

Adade CM, Oliveira IRS, Pais JAR, Souto-Padrón T (2013) Melittin peptide kills *Trypanosoma cruzi* parasites by inducing diferent cell death pathways. Toxicon 69:227–239. https://doi.org/10.1016/j.toxicon.2013.03.011

Adamczak R, Porollo A, Meller J (2005) Combining prediction of secondary structure and solvent accessibility in proteins. Proteins Struct Funct Bioinf 59(3):467–475. https://doi.org/10.1002/prot.20441

Andrä J, Berninghausen O, Leippe M (2001) Cecropins, antibacterial peptides from insects and mammals, are potently fungicidal against *Candida albicans*. Med Microbiol Immunol 189(3):169–173. https://doi.org/10.1007/s430-001-8025-x

Andrä J, Leippe M (1999) Candidacidal activity of shortened synthetic analogs of amoebapores and NK-lysin. Med Microbiol Immunol 188(3):117–124. https://doi.org/10.1007/s004300050113

Awouafack MD, McGaw LJ, Gottfried S, Mbouangouere R, Tane P, Spiteller M, Eloff JN (2013) Antimicrobial activity and cytotoxicity of the ethanol extract, fractions and eight compounds isolated from *Eriosema robustum* (Fabaceae). BMC Complement Altern Med 13:289. https://doi.org/10.1186/1472-6882-13-289

Batoni G, Maisetta G, Brancatisano FL, Esin S, Campa M (2011) Use of antimicrobial peptides against microbial biofilms: advantages and limits. Curr Med Chem 18(2):256–279. https://doi.org/10.2174/092986711794088399

Brauner A, Alvendal C, Chromek M, Stopsack KH, Ehrstrom S, Schroder JM, Bohm-Starke N (2018) Psoriasin, a novel anti-*Candida albicans* adhesin. J Mol Med (berl) 96(6):537–545. https://doi.org/10.1007/s00109-018-1637-6

Chang HT, Tsai PW, Huang HH, Liu YS, Chien TS, Lan CY (2012) LL37 and hBD-3 elevate the beta-1,3-exoglucanase activity of *Candida albicans* Xog1p, resulting in reduced fungal adhesion to plastic. Biochem J 441(3):963–970. https://doi.org/10.1042/BJ20111454

Chen X, Zhang L, Wu Y, Wang L, Ma C, Xi X, Bininda-Emonds ORP, Shaw C, Chen T, Zhou M (2018) Evaluation of the bioactivity of a mastoparan peptide from wasp venom and of its analogues designed through targeted engineering. Int J Biol Sci 14(6):599–607. https://doi.org/10.7150/ijbs.23419

Cho J, Lee DG (2011) Oxidative stress by antimicrobial peptide pleurocidin triggers apoptosis in *Candida albicans*. Biochimie 93(10):1873–1879. https://doi.org/10.1016/j.biochi.2011.07.011

Choi H, Lee DG (2014) Antifungal activity and pore-forming mechanism of astacidin 1 against *Candida albicans*. Biochimie 105:58–63. https://doi.org/10.1016/j.biochi.2014.06.014

CLSI, 2017. Reference method for broth dilution antifungal susceptibility testing of yeast, 4th edition: M27, Clinical and Laboratory Standards Institute, Wayne.

Culik RM, Abaskharon RM, Pazos IM, Gai F (2014) Experimental validation of the role of trifluoroethanol as a nanocrowder. J Phys Chem B 118(39):11455–11461. https://doi.org/10.1021/jp508056w

da Silva AV, De Souza BM, Dos Santos Cabrera MP, Dias NB, Gomes PC, Neto JR, Stabeli RG, Palma MS (2014) The effects of the C-terminal amidation of mastoparans on their biological actions and interactions with membrane-mimetic systems. Biochim Biophys Acta 1838:2357–2368. https://doi.org/10.1016/j.bbamem.2014.06.012

da Silva AM, Silva-Gonçalves LC, Oliveira FA, Arcisio-Miranda M (2018) Pro-necrotic activity of cationic mastoparan peptides in human glioblastoma multiforme cells via membranolytic action. Mol Neurobiol 55(7):5490–5504. https://doi.org/10.1007/s12035-017-0782-1

Danchik C, Casadevall A (2021) Role of cell surface hydrophobicity in the pathogenesis of medically-significant fungi. Front Cell Infect Microbiol 10:594973. https://doi.org/10.3389/fcimb.2020.594973

de Lacorte Singulani J, Galeane MC, Ramos MD, Gomes PC, Dos Santos CT, de Souza BM, Palma MS, Fusco Almeida AM, Mendes Giannini MJS (2019) Antifungal activity, toxicity, and membranolytic action of a mastoparan analog peptide. Front Cell Infect Microbiol 9:419. https://doi.org/10.3389/fcimb.2019.00419

de Souza BM, da Silva AV, Resende VM, Arcuri HA, dos Santos Cabrera MP, Neto JR, Palma MS (2009) Characterization of two novel polyfunctional mastoparan peptides from the venom of the social wasp *Polybia paulista*. Peptides 30(8):1387–1395. https://doi.org/10.1016/j.peptides.2009.05.008

Do N, Weindl G, Grohmann L, Salwiczek M, Koksch B, Korting HC, Schäfer-Korting M (2014) Cationic membrane-active peptides - anticancer and antifungal activity as well as penetration into human skin. Exp Dermatol 23(5):326–331. https://doi.org/10.1111/exd.12384

do Nascimento Dias J, de Souza Silva C, de Araujo AR, Souza JMT, de Holanda Veloso Junior PH, Cabral WF, da Gloria da Silva M, Eaton P, de Souza de Almeida Leite JR, Nicola AM, Albuquerque P, Silva-Pereira I (2020) Mechanisms of action of antimicrobial peptides ToAP2 and NDBP-5.7 against *Candida albicans* planktonic and biofilm cells. Sci Rep 10(1):10327. https://doi.org/10.1038/s41598-020-67041-2

Dudiuk C, Berrio I, Leonardelli F, Morales-Lopez S, Theill L, Macedo D, Yesid-Rodriguez J, Salcedo S, Marin A, Gamarra S, Garcia-Effron G (2019) Antifungal activity and killing kinetics of anidulafungin, caspofungin and amphotericin B against *Candida auris*. J Antimicrob Chemother 74(8):2295–2302. https://doi.org/10.1093/jac/dkz178

Ellepola AN, Joseph BK, Khan ZU (2013) Changes in the cell surface hydrophobicity of oral *Candida albicans* from smokers, diabetics, asthmatics, and healthy individuals following limited exposure to chlorhexidine gluconate. Med Princ Pract 22(3):250–254. https://doi.org/10.1159/000345641

El-Wahed AA, Yosri N, Sakr HH, Du M, Algethami AFM, Zhao C, Abdelazeem AH, Tahir HE, Masry SHD, Abdel-Daim MM, Musharraf SG, El-Garawani I, Kai G, Al Naggar Y, Khalifa SAM,

El-Seedi HR (2021) Wasp venom biochemical components and their potential in biological applications and nanotechnological interventions. Toxins (Basel) 13(3):206. https://doi.org/10.3390/toxins13030206

Fazly A, Jain C, Dehner AC, Issi L, Lilly EA, Ali A, Cao H, Fidel PL Jr, Rao RP, Kaufman PD (2013) Chemical screening identifies filastatin, a small molecule inhibitor of *Candida albicans* adhesion, morphogenesis, and pathogenesis. Proc Natl Acad Sci USA 110(33):13594–13599. https://doi.org/10.1073/pnas.1305982110

Galeane MC, Gomes PC, Singulani JL, de Souza BM, Palma MS, Mendes-Giannini MJ, Almeida AM (2019) Study of mastoparan analog peptides against *Candida albicans* and safety in zebrafish embryos (Danio rerio). Future Microbiol 14:1087–1097. https://doi.org/10.2217/fmb-2019-0060

Goswami RR, Pohare SD, Raut JS, Karuppayil SM (2017) Cell surface hydrophobicity as a virulence factor in *Candida albicans*. Biosci Biotech Res Asia 14:1503–1511

Hazen KC, Hazen BW (1992) Hydrophobic surface protein masking by the opportunistic fungal pathogen *Candida albicans*. Infect Immun 60(4):1499–1508. https://doi.org/10.1128/iai.60.4.1499-1508.1992

Hilchie AL, Sharon AJ, Haney EF, Hoskin DW, Bally MB, Franco OL, Corcoran JA, Hancock RE (2016) Mastoparan is a membranolytic anti-cancer peptide that works synergistically with gemcitabine in a mouse model of mammary carcinoma. Biochim Biophys Acta 1858:3195–3204. https://doi.org/10.1016/j.bbamem.2016.09.021

Hossen S, Gan SH, Khalil I (2017) Melittin, a potential natural toxin of crude bee venom: probable future arsenal in the treatment of diabetes mellitus. J Chem 2017:1–7. https://doi.org/10.1155/2017/4035626

Indrayanto G, Putra GS, Suhud F (2021) Validation of in-vitro bioassay methods: application in herbal drug research. Profiles Drug Subst Excip Relat Methodol 46:273–307. https://doi.org/10.1016/bs.podrm.2020.07.005

Irazazabal LN, Porto WF, Ribeiro SM, Casale S, Humblot V, Ladram A, Franco OL (2016) Selective amino acid substitution reduces cytotoxicity of the antimicrobial peptide mastoparan. Biochim Biophys Acta 11:2699–2708. https://doi.org/10.1016/j.bbamem.2016.07.001

Kim Y, Son M, Noh EY, Kim S, Kim C, Yeo JH, Park C, Lee KW, Bang WY (2016) MP-V1 from the venom of social wasp *Vespula vulgaris* is a de novo type of mastoparan that displays superior antimicrobial activities. Molecules 21(4):512. https://doi.org/10.3390/molecules21040512

Kočendová J, Vaňková E, Volejníková A, Nešuta O, Buděšínský M, Socha O, Hájek M, Hadravová R, Čeřovský V (2019) Antifungal activity of analogues of antimicrobial peptides isolated from bee venoms against vulvovaginal *Candida* spp. FEMS Yeast Res 19(3):foz013. https://doi.org/10.1093/femsyr/foz013

Krausova G, Hyrslova I, Hynstova I (2019) In vitro evaluation of adhesion capacity, hydrophobicity, and auto-aggregation of newly isolated potential probiotic strains. Fermentation 5:100. https://doi.org/10.3390/fermentation5040100

Le Lay C, Akerey B, Fliss I, Subirade M, Rouabhia M (2008) Nisin Z inhibits the growth of Candida albicans and its transition from blastospore to hyphal form. J Appl Microbiol 105(5):1630–1639. https://doi.org/10.1111/j.1365-2672.2008.03908.x

Lee G, Bae H (2016) Anti-inflammatory applications of melittin, a major component of bee venom: detailed mechanism of action and adverse effects. Molecules. https://doi.org/10.3390/molecules21050616

Lee DL, Mant CT, Hodges RS (2003) A novel method to measure self-association of small amphipathic molecules: temperature profiling in reversed-phase chromatography. J Biol Chem 278(25):22918–22927. https://doi.org/10.1074/jbc.M301777200

Lee Y, Puumala E, Robbins N, Cowen LE (2021) Antifungal drug resistance: molecular mechanisms in *Candida albicans* and beyond. Chem Rev 121(6):3390–3411. https://doi.org/10.1021/acs.chemrev.0c00199

Lee H, Woo ER, Lee DG (2018) Apigenin induces cell shrinkage in *Candida albicans* by membrane perturbation. FEMS Yeast Res 18(1):foy003. https://doi.org/10.1093/femsyr/foy003

Lima WG, Batista Filho FL, Lima IP, Simião DC, Brito JCM, da CruzNizer WS, Cardoso VN, Fernandes SOA (2022) Antibacterial, anti-biofilm, and anti-adhesive activities of melittin, a honeybee venom-derived peptide, against quinolone-resistant uropathogenic *Escherichia coli* (UPEC) Nat Prod Res. https://doi.org/10.1080/14786419.2022.2032047

Lohse MB, Gulati M, Johnson AD, Nobile CJ (2018) Development and regulation of single and multi-species *Candida albicans* biofilms. Nat Rev Microbiol 16(1):19–31. https://doi.org/10.1038/nrmicro.2017.107

Lum KY, Tay ST, Le CF, Lee VS, Sabri NH, Velayuthan RD, Hassan H, Sekaran SD (2015) Activity of novel synthetic peptides against *Candida albicans*. Sci Rep 5:9657. https://doi.org/10.1038/srep09657

Lyu C, Fang F, Li B (2019) Anti-tumor effects of melittin and its potential applications in clinic. Curr Protein Pept Sci 20(3):240–250. https://doi.org/10.2174/1389203719666180612084615

Lyu Y, Yang Y, Lyu X, Dong N, Shan A (2016) Antimicrobial activity, improved cell selectivity and mode of action of short PMAP-36-derived peptides against bacteria and *Candida*. Sci Rep 6:27258. https://doi.org/10.1038/srep27258

Mayer FL, Wilson D, Hube B (2013) *Candida albicans* pathogenicity mechanisms. Virulence 4(2):119–128. https://doi.org/10.4161/viru.22913

Memariani H, Memariani M (2021) Melittin as a promising anti-protozoan peptide: current knowledge and future prospects. AMB Express 11(1):69. https://doi.org/10.1186/s13568-021-01229-1

Memariani H, Memariani M (2020) Anti-fungal properties and mechanisms of melittin. Appl Microbiol Biotechnol 104(15):6513–6526. https://doi.org/10.1007/s00253-020-10701-0

Memariani H, Memariani M, Robati RM, Nasiri S, Abdollahimajd F, Baseri Z, Moravvej H (2020) Anti-Staphylococcal and cytotoxic activities of the short anti-microbial peptide PVP. World J Microbiol Biotechnol 36(11):174. https://doi.org/10.1007/s11274-020-02948-6

Memariani H, Memariani M, Shahidi-Dadras M, Nasiri S, Akhavan MM, Moravvej H (2019) Melittin: from honeybees to superbugs. Appl Microbiol Biotechnol 103(8):3265–3276. https://doi.org/10.1007/s00253-019-09698-y

Memariani H, Shahbazzadeh D, Ranjbar R, Behdani M, Memariani M, Bagheri KP (2017) Design and characterization of short hybrid antimicrobial peptides from pEM-2, mastoparan-VT1, and mastoparan-B. Chem Biol Drug Des 89(3):327–338. https://doi.org/10.1111/cbdd.12864

Memariani H, Shahbazzadeh D, Sabatier JM, Pooshang Bagheri K (2018) Membrane-active peptide PV3 efficiently eradicates multidrug-resistant *Pseudomonas aeruginosa* in a mouse model of burn infection. APMIS 126(2):114–122. https://doi.org/10.1111/apm.12791

Mohamed MF, Abdelkhalek A, Seleem MN (2016) Evaluation of short synthetic antimicrobial peptides for treatment of drug-resistant and intracellular *Staphylococcus aureus*. Sci Rep 6:29707. https://doi.org/10.1038/srep29707

Moreno M, Giralt E (2015) Three valuable peptides from bee and wasp venoms for therapeutic and biotechnological use: melittin, apamin and mastoparan. Toxins (basel) 7(4):1126–1150. https://doi.org/10.3390/toxins7041126

Nobile CJ, Johnson AD (2015) *Candida albicans* biofilms and human disease. Annu Rev Microbiol 69:71–92. https://doi.org/10.1146/annurev-micro-091014-104330

Olsen I (2015) Biofilm-specific antibiotic tolerance and resistance. Eur J Clin Microbiol Infect Dis 34(5):877–886. https://doi.org/10.1007/s10096-015-2323-z

Park C, Lee DG (2009) Fungicidal effect of antimicrobial peptide arenicin-1. Biochim Biophys Acta 1788(9):1790–1796. https://doi.org/10.1016/j.bbamem.2009.06.008

Park SC, Kim JY, Kim EJ, Cheong GW, Lee Y, Choi W, Lee JR, Jang MK (2018) Hydrophilic linear peptide with histidine and lysine residues as a key factor affecting antifungal activity. Int J Mol Sci 19(12):3781. https://doi.org/10.3390/ijms19123781

Porto WF, Irazazabal L, Alves ESF, Ribeiro SM, Matos CO, Pires ÁS, Fensterseifer ICM, Miranda VJ, Haney EF, Humblot V, Torres MDT, Hancock REW, Liao LM, Ladram A, Lu TK, de la Fuente-Nunez S, Franco OC (2018) In silico optimization of a guava antimicrobial peptide enables combinatorial exploration for peptide design. Nat Commun 9(1):1490. https://doi.org/10.1038/s41467-018-03746-3

Raja Z, André S, Abbassi F, Humblot V, Lequin O, Bouceba T, Correia I, Casale S, Foulon T, Sereno D, Oury B, Ladram A (2017) Insight into the mechanism of action of temporin-SHa, a new broad-spectrum antiparasitic and antibacterial agent. PLoS ONE 12(3):e0174024. https://doi.org/10.1371/journal.pone.0174024

Reen FJ, Phelan JP, Gallagher L, Woods DF, Shanahan RM, Cano R, Eoin M, McGlacken GP, Oara F (2016) Exploiting interkingdom interactions for development of small-molecule inhibitors of *Candida albicans* biofilm formation. Antimicrob Agents Chemother 60(10):5894–5905. https://doi.org/10.1128/AAC.00190-16

Rončević T, Puizina J, Tossi A (2019) Antimicrobial peptides as anti-infective agents in pre-post-antibiotic era? Int J Mol Sci 20 (22). https://doi.org/10.3390/ijms20225713

Scarsini M, Tomasinsig L, Arzese A, D'Este F, Oro D, Skerlavaj B (2015) Antifungal activity of cathelicidin peptides against planktonic and biofilm cultures of *Candida* species isolated from vaginal infections. Peptides 71:211–221. https://doi.org/10.1016/j.peptides.2015.07.023

Silva ON, Torres MDT, Cao J, Alves ESF, Rodrigues LV, Resende JM, Liao LM, Porto WF, Fensterseifer ICM, Lu TK, Franco OL, de la Fuente-Nunez C (2020) Repurposing a peptide toxin from wasp venom into antiinfectives with dual antimicrobial and immunomodulatory properties. Proc Natl Acad Sci USA 117(43):26936–26945. https://doi.org/10.1073/pnas.2012379117

Singleton DR, Fidel PL Jr, Wozniak KL, Hazen KC (2005) Contribution of cell surface hydrophobicity protein 1 (Csh1p) to virulence of hydrophobic *Candida albicans* serotype A cells. FEMS Microbiol Lett 244(2):373–377. https://doi.org/10.1016/j.femsle.2005.02.010

Smart SS, Mason TJ, Bennell PS, Maeij NJ, Geysen HM (1996) High-throughput purity estimation and characterisation of synthetic peptides by electrospray mass spectrometry. Int J Pept Protein Res 47(1–2):47–55. https://doi.org/10.1111/j.1399-3011.1996.tb00809.x

Snyder SS, Gleaton JW, Kirui D, Chen W, Millenbaugh NJ (2021) Antifungal activity of synthetic scorpion venom-derived peptide analogues against *Candida albicans*. Int J Pept Res Ther 27:281–291. https://doi.org/10.1007/s10989-020-10084-w

Talapko J, Juzbasic M, Matijevic T, Pustijanac E, Bekic S, Kotris I, Skrlec I (2021) *Candida albicans*—the virulence factors and clinical manifestations of infection. J Fungi (Basel) 7(2):79. https://doi.org/10.3390/jof7020079

Tan L, Bai L, Wang L, He L, Li G, Du W, Shen T, Xiang Z, Wu J, Liu Z, Hu M (2018) Antifungal activity of spider venom-derived peptide lycosin-I against *Candida tropicalis*. Microbiol Res 216:120–128. https://doi.org/10.1016/j.micres.2018.08.012

Tsai PW, Yang CY, Chang HT, Lan CY (2011) Human antimicrobial peptide LL-37 inhibits adhesion of *Candida albicans* by interacting with yeast cell-wall carbohydrates. PLoS ONE 6(3):e17755. https://doi.org/10.1371/journal.pone.0017755

Tsang PW, Bandara HM, Fong WP (2012) Purpurin suppresses *Candida albicans* biofilm formation and hyphal development. PLoS ONE 7(11):e50866. https://doi.org/10.1371/journal.pone.0050866

Uddin MB, LeeBH NC, Kim JH, Kim TH, Lee HC, Kim CG, Lee JS, Kim CJ (2016) Inhibitory effects of bee venom and its components against viruses in vitro and in vivo. J Microbiol 54(12):853–866. https://doi.org/10.1007/s12275-016-6376-1

Vaňková E, Kašparová P, Dulíčková N, Čeřovský V (2020) Combined effect of lasioglossin LL-III derivative with azoles against *Candida albicans* virulence factors: biofilm formation, phospholipases, proteases and hemolytic activity. FEMS Yeast Res 20(3):foaa020. https://doi.org/10.1093/femsyr/foaa020

Vila-Farrés X, López-Rojas R, Pachón-Ibánez ME, Teixidó M, Pachón J, Vila J, Giralt E (2015) Sequence-activity relationship, and mechanism of action of mastoparan analogues against extended-drug resistant *Acinetobacter baumannii*. EurJ Med Chem 101:34–40. https://doi.org/10.1016/j.ejmech.2015.06.016

Vrablikova A, Czernekova L, Cahlikova R, Novy Z, Petrik M, Imran S, Novak Z, Krupka M, Cerovsky V, Turanek J, Raska M (2017) Lasioglossins LLIII affect the morphogenesis of *Candida albicans* and reduces the duration of experimental vaginal candidiasis in mice. Microbiol Immunol 61(11):474–481. https://doi.org/10.1111/1348-0421.12538

Walsh TJMD, Hayden RT, Larone DH (2018) Larone's medically important fungi: a guide to identification, 6th edn. ASM Press, Washington, DC

Wang K, Yan J, Dang W, Xie J, Yan B, Yan W, Sun M, Zhang B, Ma M, Zhao Y, Jia F, Zhu R, Chen W, Wang R (2014) Dual antifungal properties of cationic antimicrobial peptides polybia-MPI: membrane integrity disruption and inhibition of biofilm formation. Peptides 56:22–29. https://doi.org/10.1016/j.peptides.2014.03.005

Yang X, Wang Y, Lee WH, Zhang Y (2013) Antimicrobial peptides from the venom gland of the social wasp *Vespa tropica*. Toxicon-omy 74:151–157. https://doi.org/10.1016/j.toxicon.2013.08.056